Journal of Applied Polymer Science

# Preparation of polysiloxane phosphonic acid doped polybenzimidazole high-temperature proton-exchange membrane

**Huilin Li, Chunhui Shen, Shanshan Yin, Wei Li**
Department of Polymer Materials and Engineering, School of Material Science and Engineering, Wuhan University of Technology, 122 Luoshi Road, Wuhan 430070, People's Republic of China
Correspondence to: C. Shen (E-mail: shenchunhui@whut.edu.cn)

**ABSTRACT:** Polysiloxane phosphonic acid doped polybenzimidazole (PBI) high-temperature membranes were fabricated in this study. Polysiloxane phosphonic acid instead of phosphoric acid was used as a proton conductor to prevent acid from leaking. The membrane samples with different amounts of PBI were prepared and characterized with respect to the structure, thermal properties, oxidative stability, proton conductivity, and mechanical properties. The Fourier transform infrared results show that hydrogen bonds formed between PBI and polysiloxane phosphonic acid. Thermal analysis confirmed that the temperature at which membrane experienced 10% weight loss was above 230°C. None of the membrane samples broke into pieces after Fenton reagent testing. The proton conductivity of the membrane samples with 5% PBI was up to 0.034 S/cm at 140°C under nominally anhydrous conditions. The tensile strength of the membrane samples with 10% PBI was 18.3 MPa. © 2015 Wiley Periodicals, Inc. J. Appl. Polym. Sci. **2016**, *133*, 42956.

**KEYWORDS:** crosslinking; dendrimers; electrochemistry; gels; hyperbranched polymers and macrocycles

Received 28 May 2015; accepted 16 September 2015
**DOI: 10.1002/app.42956**

## INTRODUCTION

Proton-exchange membrane fuel cells (PEMFCs) are one of the most promising clean energy-shift devices, and proton-exchange membranes (PEMs) are one of the key components of PEMFCs. The PEM serves two functions, namely, (1) to separate $H_2$ from $O_2$ to prevent cross-permeation and (2) to transport the protons toward a specific direction. Currently, the most commonly used PEM for PEMFCs is a perfluorosulfonic acid-type membrane, such as Nafion, which contains sulfonic groups as protogenic groups (to donate protons) and water as a proton solvent (to transport protons via a vehicle mechanism). This kind of PEM is thermally and mechanically stable. The proton conductivity is high ($10^{-1}$ S/cm) when the operation temperature is under 80°C. In fact, the proton conductivity of Nafion is very dependent on the water content of the membrane.[1–3] As we all know, the proton conductivity of Nafion falls sharply when the operation temperature is above 80°C; this is due to the evaporation of moisture.[4] The limited operating conditions complicate the water and heat management of PEMFC; in the meantime, high-purity hydrogen is required to prevent the poisoning of electrodes by CO. Therefore, a new type of PEM that possesses a high proton conductivity under high-temperature and low-relative-humidity conditions is considered to be one of the keys to the application of high-temperature PEMFCs.[5] High-temperature PEMFCs (a high temperature refers here to a temperature range from 100 to 150°C) has attracted extensive attention because of several benefits, such as their higher power efficiency, simplified cooling device, and increased reaction velocity.[6]

The study of hybrid membranes of silane and phosphoric acid began early.[7–13] A membrane that was synthesized by epoxycyclohexylethyltrimethoxysilane (EHTMS) and amino trimethylene phosphonic acid (ATMP) was also reported by our team.[14] EHTMS hydrolysis and crosslinking in the presence of ATMP were accompanied by the ring-opening reaction of epoxy; thus, ATMP was bonded to the EHTMS. This kind of membrane showed a high proton conductivity under high-temperature and nominally anhydrous conditions, but the membrane was too fragile. We hope to improve the mechanical properties and oxidative stability of the membrane by introducing a polymer matrix.[15] Acid-doped polybenzimidazole (PBI) membranes have received a lot of attention recently. On the basis of our preceding works,[14,16,17] a polysiloxane phosphonic acid doped PBI membrane was examined in this study.

PBIs are a large family of aromatic heterocyclic polymers containing an imidazole ring. In this study, PBI refers to poly[2, 2′-*m*-(phenylene)−5,5′-bibenzimidazole]. PBI possesses —NH— and —N= hydrogen-bonding sites, which exhibit specific interactions with polar solvents, for example, *N,N*-dimethylacetamide (DMAc).[18] PBI is amphoteric in the sense that it behaves

as a proton donor and proton acceptor; this results in the formation of a high concentration of protonic defects because of self-dissociation.[19] PBI, the polymer matrix, helps to improve the thermal stability and mechanical performance of membranes.[20] Two methods have been reported to prepare acid-doped PBI membranes; these are the (1) fabrication of membranes from polar solvent solutions followed by soaking in a phosphoric acid solution and (2) fabrication via a sol–gel method by direction of the dissolution of PBI and phosphoric in polar solvent.[21] In this study, we adopted the second preparation method.

In this study, a comparative study of polysiloxane phosphonic acid doped PBI membranes was conducted to investigate their structure and properties. Polysiloxane phosphonic acid was formed by hydrolysis and condensation. We expected that ATMP was bonded to EHTMS. Then, a new type of membrane was prepared via the sol–gel process from PBI and polysiloxane phosphonic acid. We expected that PBI would offer a good mechanical strength, whereas the imidazole ring would help to form hydrogen bonds. The properties of the membranes were adjusted by changes in the content of PBI. The influence of the PBI content on the membrane properties, such as thermal stability, chemical stability, mechanical properties, ion-exchange capacity (IEC), and proton conductivity, was investigated.

## EXPERIMENTAL

### Materials

DMAc and ATMP were purchased from Shandong Huayou Chemistry Co., Ltd. Poly[2,2′-*m*-(phenylene)−5,5′-bibenzimidazole] was purchased from Shanghai Shengxin Plastic Products Co., Ltd. EHTMS was obtained from Aladdin. All chemicals were used as received without any further purification.

### Preparation of Polysiloxane Phosphonic Acid

The polysiloxane phosphonic acid was prepared from EHTMS and ATMP by the sol–gel method. The EHTMS/ATMP molar ratio was 1:0.5. In a 50-mL glass beaker, EHTMS was dissolved in DMAc (15 mL) at ambient temperature, and ATMP was added slowly to this solution and was followed by stirring for 3 h and aging for 3 days at ambient temperature. Then, the colorless, transparent polysiloxane phosphonic acid sol was obtained.

### Preparation of the Membranes

PBI was dissolved in DMAc (10 mL) in a 25-mL glass beaker. The polysiloxane phosphonic acid was added to the solution dropwise; this was followed by stirring for 12 h at ambient temperature. The mixture was cast onto a Teflon mold and dried in a vacuum oven at 80°C for 48 h and 120°C for 4 h to remove the solvent. The membrane was peeled off of the Teflon mold. A membrane with a thickness of 0.05–0.5 mm was prepared. In this synthesis, three membrane samples with PBI/polysiloxane phosphonic acid weight ratios of 5:95, 10:90, and 90:10 were prepared; these contained 5, 10, and 90% PBI, respectively.

### Characterization

Fourier transform infrared (FTIR) spectra of the membrane samples were recorded on a Nicolet 170SX FTIR spectrometer (4000–500 $cm^{-1}$, resolution = 4 $cm^{-1}$). The studies were carried out at ambient temperature on the samples. The X-ray diffraction (XRD) patterns of the sample powders were collected on a Rigaku D/MAX-RB powder diffraction apparatus with Cu Kα radiation. Thermogravimetric analysis measurements were conducted with a Netzsch STA499C instrument at a heating rate of 10°C/min under air flowing at 20 mL/min. The proton conductivity of the polysiloxane phosphonic acid doped PBI membranes was measured with a four-point-probe conductivity cell attached to an electrochemical impedance spectrometer (Autolab PG30/FRA, Eco Chemie, The Netherlands) from 1 Hz to 10 kHz. The proton conductivity ($\sigma$) was calculated from the following equation:

$$\sigma = l/Rwd$$

where $l$, $w$, and $d$ are the distance between the two electrodes, membrane width, and thickness, respectively.[22] The oxidative stability of the membrane samples was examined by the immersion of the samples in Fenton reagent (3% hydrogen peroxide solution containing 2-ppm $Fe^{2+}$) at 80°C.

IEC of the membrane was measured by a titration method. The membrane samples were immersed into distilled water for different soaking times; this was followed by soaking in a saturated NaCl solution for 7 days to replace $H^+$ with $Na^+$ in the membranes. Then, the remaining solution was titrated with NaOH solution (0.01 mol/L). The IEC was calculated from the following equation:

$$\text{IEC (mmol/g)} = C_{\text{NaOH}} \times V_{\text{NaOH}} / W_{\text{dry}}$$

where $C_{\text{NaOH}}$ and $V_{\text{NaOH}}$ are the concentration (mol/L) and volume of NaOH solution (mL), respectively, and $W_{\text{dry}}$ (g) is the weight of the dry membrane sample.

The activation energy ($E_a$) of the proton conductivity of the membrane samples was calculated from an Arrhenius equation:

$$\sigma = \sigma \exp\left(-\frac{Ea}{kT}\right)$$

where $\sigma_0$ is a pre-exponential factor, $k$ is Boltzmann's constant ($1.38 \times 10^{-23}$ J/k), and $T$ is the Kelvin temperature (K).

The mechanical properties of the membrane samples were analyzed by uniaxial tension testing, and the test was performed on a CMT6503 universal testing machine (SANS, Shenzhen, China) at room temperature. Membrane samples were designed to be rectangular (10 × 50 $mm^2$). The average value of the tensile strength of the membranes was obtained from three tests for every membrane sample.

## RESULTS AND DISCUSSION

### FTIR Analysis of the Membranes

Before FTIR characterization, the membrane samples were boiled in boiling water for 24 h and dried in a vacuum oven to remove DMAc and unbound ATMP. The FTIR spectra of the pristine PBI membrane, 90% PBI membrane, 10% PBI membrane, and 5% PBI membrane are presented in Figure 1. The absence of O—H stretching of $H_2O$ around 3616 $cm^{-1}$ in all of the spectra indicated the efficiency of the drying process.[23] From the spectrum of the pristine PBI shown in Figure 1(a), the absorption at 3432 $cm^{-1}$ was attributed to the free N—H

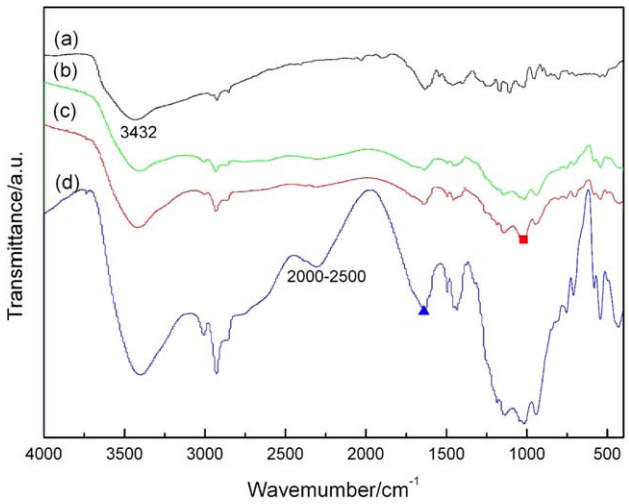


**Figure 1.** FTIR spectra of the membranes: (a) pristine PBI membrane, (b) 90% PBI membrane, (c) 10% PBI membrane, and (d) 5% PBI membrane. [Color figure can be viewed in the online issue, which is available at wileyonlinelibrary.com.]

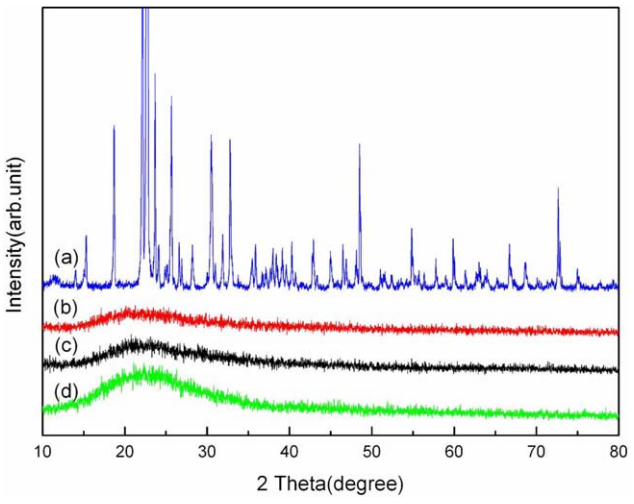


**Figure 3.** XRD patterns of ATMP and the membranes: (a) ATMP, (b) 90% PBI membrane, (c) 10% PBI membrane, and (d) 5% PBI membrane. [Color figure can be viewed in the online issue, which is available at wileyonlinelibrary.com.]

stretching vibrations of the benzimidazole ring. However, the peak that existed in Figure 1(b–d) shifted gradually to a low-frequency region with increasing content of polysiloxane phosphonic acid in the membrane. In addition, the absorption at 1632cm$^{-1}$ (marked with a solid triangle) was attributed to C═N in the benzimidazole ring. The 1632-cm$^{-1}$ peak that is also shown in Figure 1(b–d) only shifted gradually to the high-frequency region with increasing polysiloxane phosphonic acid. These changes may have been due to the formation of hydrogen bonds between N—H, C═N, and P═O or P—OH.

The FTIR spectra of the membranes are presented in Figure 1(b–d) for comparison. Two peaks at 822 and 1091 cm$^{-1}$, which corresponded to the methoxy stretching vibrations of Si—$OCH_3$ and Si—O stretching vibrations,[9] were absent the spectra shown in Figure 1(b–d). At the same time, the peaks at 1000–1100 cm$^{-1}$ (marked with a solid square), which were attributed to Si—O—Si stretching vibrations, existed in the spectra shown in Figure 1(b–d). These facts indicate that the siloxane groups of EHTMS underwent hydrolysis and a condensation reaction,[7] and the Si—$OCH_3$ was converted into an Si—O—Si network.[16] The peak at 890 cm$^{-1}$ attributed to antisymmetric deformation of the epoxy group was absent the spectra in Figure 1(b–d); this suggests that the epoxy group appeared to undergo a ring-opening reaction, and the ATMP was probably bonded to a three-dimensional Si—O—Si network. However, it was difficult to determine how much ATMP was bonded to the Si—O—Si network. Figure 1(d) showed the strongest peak at 2000–2500 cm$^{-1}$; this was attributed to the P—OH group and indicated that the increase in polysiloxane phosphonic acid in the membrane samples caused the increase of the P—OH group. The possible structure of the membrane is shown in Figure 2.

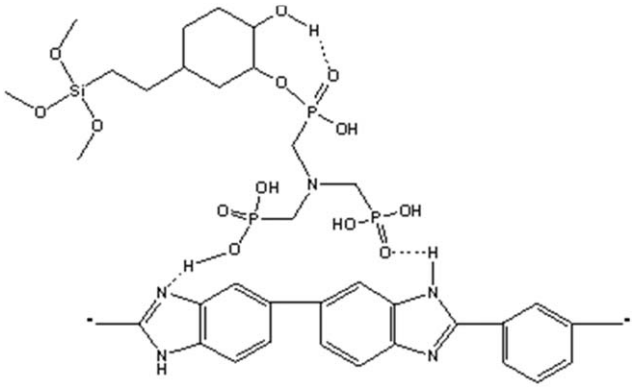

**Figure 2.** Possible structure of the membrane (dashed lines represent the hydrogen bonds).

### XRD Analysis of the Membranes

The XRD patterns of the ATMP particles and membrane samples are shown in Figure 3. PBI was amorphous in nature, whereas ATMP was crystalline, as shown in Figure 3(a). Thus, the XRD pattern of ATMP particles showed some sharp peaks. The XRD patterns of membranes presented only a weak broad peak in the region of 2$\theta$ from 15 to 35°; this was attributed to the coherent diffraction of the Si—O—Si backbone of polysiloxane phosphonic acid.[24] This indicates that the membrane samples were almost amorphous. In comparison with Figure 3(b–d), there was a relatively obvious peak in the region of 2$\theta$ from 15 to 35°; this may have been due to the large amount of polysiloxane phosphonic acid, which contained an Si—O—Si network. In addition, the XRD patterns of the membrane samples did not show any characteristic peak of ATMP, and this suggested that ATMP was bonded to EHTMS. These results were in accordance with FTIR analysis.

### Thermal Analysis of the Membranes

The thermogravimetric curves of the membrane samples are shown in Figure 4. For the pure PBI membrane, from 50 to 400°C, the weight loss was less than 10%, and the weight loss was mainly due to the evaporation of moisture and residual solvents. The weight loss at 80°C was assigned to the evaporation

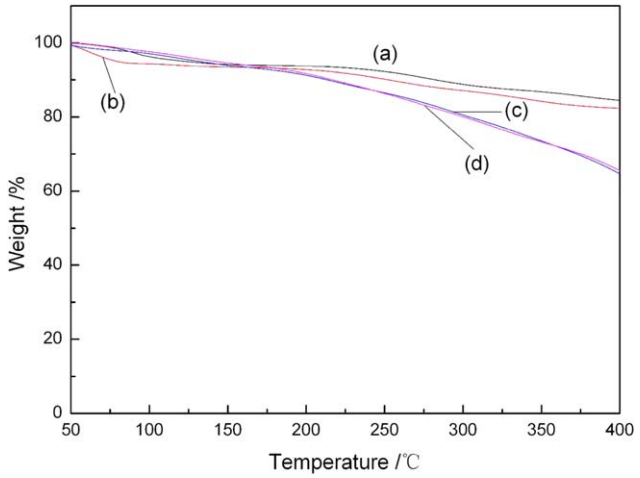


**Figure 4.** Thermogravimetric curves of the membranes: (a) pristine PBI membrane, (b) 90% PBI membrane, (c) 10% PBI membrane, and (d) 5% PBI membrane. [Color figure can be viewed in the online issue, which is available at wileyonlinelibrary.com.]

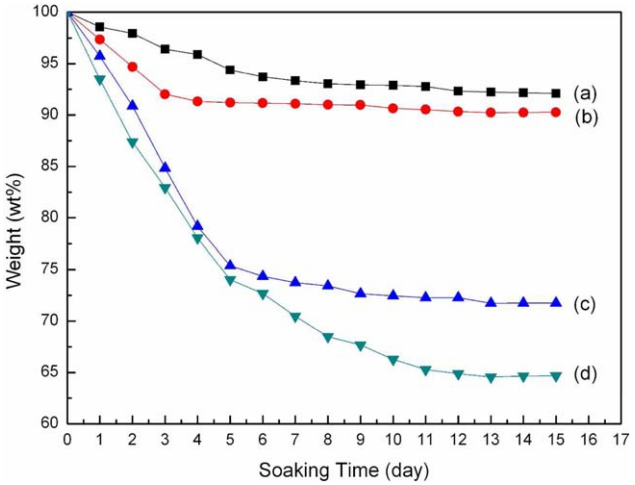


**Figure 5.** Effect of the membrane soaking time in a Fenton reagent at 80°C on the weight loss of the membranes: (a) pristine PBI membrane, (b) 90% PBI membrane, (c) 10% PBI membrane, and (d) 5% PBI membrane. [Color figure can be viewed in the online issue, which is available at wileyonlinelibrary.com.]

of moisture for all of the curves. As shown in Figure 4(b–d), a 6% mass loss occurred in the temperature range of 90–150°C and was due the evaporation of bonded water. A high temperature would result in the condensation of unbound ATMP.[16] So, the weight loss at 250–330°C may have been due to the condensation of $P(O)(OH)_2$ for Figure 4(b–d). As also shown in Figure 4, the thermal stability of the membrane increased with increasing PBI; this showed better thermal properties than those observed in our previous polysiloxane phosphonic acid membrane.[14] This suggested that the PBI matrix improved the thermal stability of the membrane. In addition, the temperature at which the membrane experienced 10% weight loss ($T_{10\%}$) is shown in Table I. As shown in Table I, the 5 and 10% PBI membranes still showed good thermal stability because their $T_{10\%}$ was above 230°C.

### Oxidative Stability of the Membranes

The oxidative stability of a membrane is very important to the lifetime of PEMFCs, and Fenton reagent is commonly used to test the oxidative stability of membranes. The effect of the membrane soaking time in Fenton reagent at 80°C on the weight loss of the membrane is shown in Figure 5. As shown in Figure 5(a), the weight loss of 7.895% was caused by the loss of residual solvents. During the first 5 days, weight losses of 8.7, 24.623, and 25.977%, shown in Figure 5(b–d), were due to the leaching of unbound ATMP. The weight losses of 5 and 10% PBI membrane after 5 days was due to the Si—O—Si network dissolving in Fenton reagent; this was caused by ·OH or ·OOH radical attack on the C—O—Si bonds. On the whole, 35.315, 28.241, 9.732, and 7.895% weight losses occurred for the 5, 10, and 90% PBI membranes, respectively, and the pristine PBI membrane when the membrane was exposed to Fenton reagent at 80°C. The weight losses of the membranes decreased with increasing PBI; this suggested that the introduction of PBI improved the oxidative stability of the membranes. It was interesting that all of the membrane samples did not break into pieces after 15 days; this suggested good chemical stability in the membrane samples.

**Table I.** $T_{10\%}$, $E_a$, and Tensile Strength Values of the Membranes

| Membrane | $T_{10\%}$ (°C) | $E_a$ (eV) | Tensile strength (MPa) |
|---|---|---|---|
| 90% PBI | 291 | 0.2 | 97.5 |
| 10% PBI | 278 | 0.11 | 18.3 |
| 5% PBI | 243 | 0.179 | 7.8 |

In addition, the residual amounts of polysiloxane phosphonic acid were 8.158, 69.654, and 67.58% after 15 days, respectively, for the 90, 10, and 5% PBI membranes, respectively. It was interesting that the 10% PBI membrane contained more polysiloxane phosphonic acid than the 5% PBI membrane after 15 days. Probably, the greater the amount of PBI in the membrane was, the more polysiloxane phosphonic acid was immobilized by hydrogen bonds between the benzimidazole ring and P—OH.

### IECs of the Membranes

The IECs of the membrane samples with different soaking times in distilled water are shown in Figure 6. IEC decreased with increasing PBI in the membrane; this was due to the decrease in the proton conductivity. IEC also decreased with increasing soaking time in distilled water; this was due to the leaching of unbound ATMP. After the leaching of ATMP, IEC tended to be stable for a specific sample with different soaking times. IECs of the membranes were 1.067, 0.78, and 0.06 mmol/g after 15 days, respectively, for the 5, 10, and 90% PBI membranes, respectively. The IECs of the 5 and 10% PBI membranes were close to that of the Nafion membrane (0.89 m mol/g).

### Proton Conductivity of the Membranes

Before proton conductivity characterization, the membrane samples were exposed to distilled water for 7 days and dried in a vacuum oven to remove unbound ATMP. The impedance

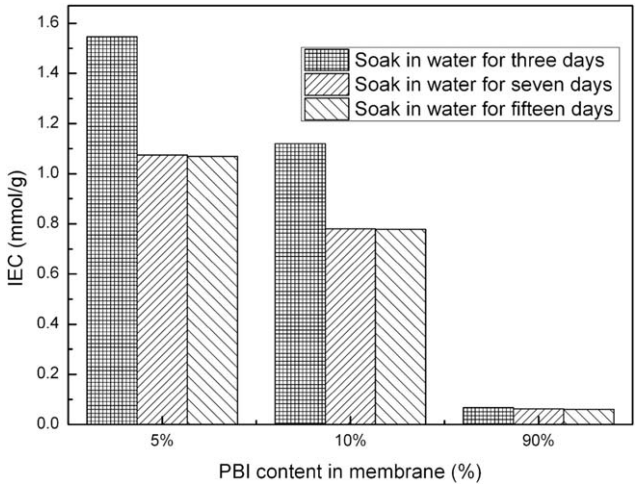


**Figure 6.** IECs of the membranes (5, 10, and 90% PBI membranes) with different soaking times in distilled water.

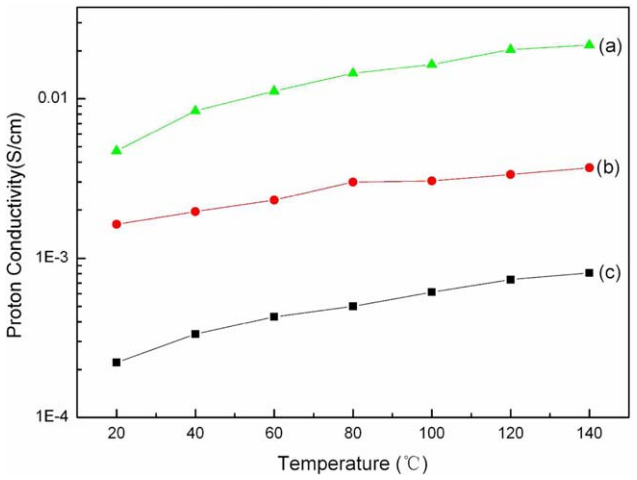


**Figure 8.** Temperature dependence of the proton conductivity (nominally anhydrous) for the membranes: (a) 5% PBI membrane, (b) 10% PBI membrane, and (c) 90% PBI membrane. [Color figure can be viewed in the online issue, which is available at wileyonlinelibrary.com.]

spectra of the 10% PBI membrane sample as a representative are shown in Figure 7. As the temperature increased, the impedance spectrum shifted to a lower resistance. The result shows that the resistance was reduced with increasing temperature.

The proton conductivity of the membrane samples under nominally anhydrous conditions at different temperatures is shown in Figure 8. As shown in Figure 8, the proton conductivity increased with increasing polysiloxane phosphonic acid; this was attributed to the dynamic hydrogen-bond network among phosphate groups. In particular, the 5% PBI membrane showed excellent proton conductivity of more than 0.01 S/cm above 40°C. As we all know, proton conduction is a thermally activated process. The proton conductivity increased with increasing temperature. For the 5% PBI membrane sample, the proton conductivity increased by almost an order of magnitude over the temperature range 20–140°C up to a maximum of 0.034 S/cm at 140°C under nominally anhydrous conditions.

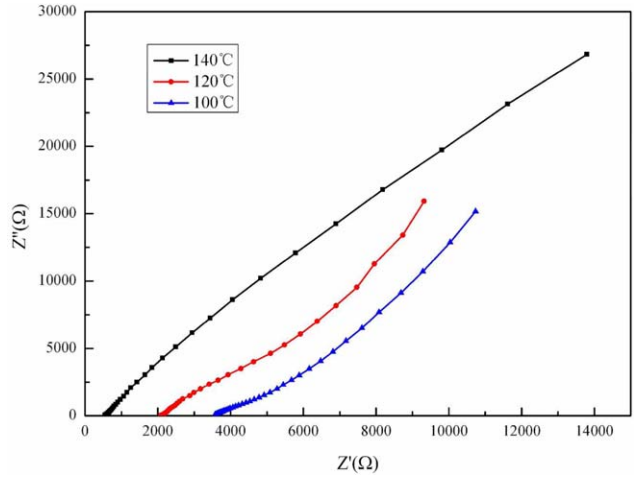


**Figure 7.** Impedance spectra of the 10% PBI membrane at 100, 120, and 140°C under nominally anhydrous conditions. [Color figure can be viewed in the online issue, which is available at wileyonlinelibrary.com.]

The $E_a$ values of the proton conductivity for the membrane samples are shown in Table I. As shown in Table I, the $E_a$ of all the membranes were around 0.1–0.4 eV, and the 10% PBI membrane had a lower $E_a$. As it is known, a low $E_a$ is favorable for proton conduction. However, the proton conductivity of the 10% PBI membrane was lower than that of the 5% PBI membrane; this needs further research.

### Mechanical Properties of the Membranes

The mechanical properties of the membranes were briefly measured, and the tensile strength of the membranes is shown in Table I. As shown in Table I, the introduction of PBI improved the tensile strength of the membranes, and the synthesized membranes showed better mechanical properties than those shown in our previous report.[14] Although the 5% PBI membrane showed a high proton conductivity, its tensile strength needed to be improved. The 10% PBI membrane showed a relatively high tensile strength (18.3 MPa). However, an appropriate PBI content in the membranes needs to be investigated further with both the proton conductivity and mechanical properties taken into account.

## CONCLUSIONS

Polysiloxane phosphonic acid doped PBI high-temperature PEMs have been successfully prepared from ATMP, PBI, and EHTMS. The FTIR spectroscopy and XRD indicated that the ATMP was partly bonded to EHTMS, and the membranes were amorphous. The proton conductivity of the membranes increased with increasing temperature or decreasing PBI in the membranes and reached 0.034S/cm under at 140°C under nominally anhydrous conditions for the 5% PBI membrane. However, the appropriate PBI content in the membranes needs to be investigated more with both the proton conductivity and mechanical properties taken into account. Compared with the membranes prepared in our previous study, the mechanical properties, oxidative stability, and thermal stability of the synthesized membranes were improved with the introduction of

PBI. Thus, PEMFCs with these membranes may be suitable for the use in the high-temperature range 100–200°C.

## ACKNOWLEDGMENTS

This work was financially supported by the National Natural Science Foundation of China (contract grant numbers 21276202 and 21076167).

## REFERENCES

1. Linas, V.; Mark, E. T.; Gabriel, B.; Stephen, J. P.; Klaus-Dieter, K. *Nat. Chem.* **2012**, *4*, 461.
2. Robert, G. *Solid State Nucl. Magn. Reson.* **2011**, *40*, 127.
3. Li, Q. F.; Rudbeck, H. C.; Chromik, A.; Jensen, J. O.; Pan, C.; Steenberg, T.; Calverley, M.; Bjerrum, N. J.; Kerres, J. *J. Membr. Sci.* **2010**, *347*, 260.
4. Chen, Y.; Thorn, M.; Christensen, S.; Versek, C.; Ambata Poe, C.; Hayward, R.; Tuominen, M. T.; Thayumanavan, S. *Nat. Chem.* **2010**, *2*, 503.
5. Jin, Y. G.; Qiao, S. Z.; Xu, Z. P.; Yan, Z.; Huang, Y.; da Costa, J. C. D.; Lu, G. Q. *J. Mater. Chem.* **2009**, *19*, 2363.
6. Shen, C.; Guo, Z.; Chen, C.; Gao, S. *J. Appl. Polym. Sci.* **2012**, *126*, 954.
7. Tadanaga, K.; Yoshida, H.; Matsuda, A.; Minami, T.; Tatsumisago, M. *Solid State Ionics* **2005**, *176*, 2997.
8. Li, S.; Zhou, Z.; Abernathy, H.; Liu, M.; Li, W.; Ukai, J.; Hase, K.; Nakanishi, M. *J. Mater. Chem.* **2006**, *16*, 858.
9. Masaki, K.; Shingo, K.; Wataru, S.; Toshinobu, Y. *Electrochim. Acta* **2007**, *52*, 5924.
10. Jin, Y.; Qiao, S.; da Costa, J. C. D.; Barry, J. W.; Bradley, P. L.; Lu, G. Q. *Adv. Funct. Mater.* **2007**, *17*, 3304.
11. Hiroshi, O.; Masaki, K.; Tetsuo, S.; Wataru, S.; Toshinobu, Y. J. *Sol–Gel Sci. Technol.* **2008**, *46*, 107.
12. Lakshminarayana, G.; Nogami, M. *Electrochim. Acta* **2009**, *54*, 4731.
13. Junji, U.; Makoto, M.; Wataru, S.; Toshinobu, Y. *Electrochim. Acta* **2009**, *55*, 298.
14. Chen, C.; Shen, C.; Kong, G.; Gao, S. *Mater. Chem. Phys.* **2013**, *140*, 24.
15. Ronghuan, H.; Qingfeng, L.; Jens Oluf, J.; Bjerrum, N. J. J. *Polym. Sci. Part A: Polym. Chem.* **2007**, *45*, 2989.
16. Kong, G.; Guo, Z.; Shen, C.; Chen, C. *J. Sol–Gel Sci. Technol.* **2013**, *66*, 84.
17. Shen, C.; Kong, G.; Wang, J.; Zhang, X. *Int. J. Hydrogen Energy* **2015**, *40*, 363.
18. Shogbon, C. B.; Brousseau, J. L.; Zhang, H.; Benicewicz, B. C.; Akpalu, Y. *Macromolecules* **2006**, *39*, 9409.
19. Steininger, H.; Schuster, M.; Kreuer, K. D.; Kaltbeitzel, A.; Binggol, B.; Meyer, W. H.; Schauff, S.; Brunklaus, G.; Maier, J.; Spiess, H. W. *Phys. Chem. Chem. Phys.* **2007**, *9*, 1764.
20. Fosca, C.; Anne, M.; Vito Di, N.; Carsten, K.; Werner, L.; Detlef, S. *Phys. Chem. Chem. Phys.* **2012**, *14*, 10022.
21. Mohamed, R. B.; Tsuyohiko, F.; Kazunari, S.; Naotoshi, N. *Sci. Rep.* **2013**, *3*, 1764.
22. Hsu, S.-L. C.; Lin, Y.-C.; Tasi, T.-Y.; Jheng, L.-C.; Shen, C.-H. *J. Appl. Polym. Sci.* **2013**, *130*, 4107.
23. Arindam, S.; Dhamodaran, A.; Murali Sankar, R.; Tushar, J. J. *Mater. Chem. B* **2007**, *111*, 12124.
24. Labato, J.; Canizares, P.; Rodrigo, M. A.; Ruiz-Lopez, C.; Linares, J. J. *J. Appl. Electrochem.* **2008**, *38*, 793.